



All-in-fiber SESAM based comb oscillator with an intra-cavity electro-optic modulator for coherent high bandwidth stabilization

S. M. SCHWEYER,^{1,2,3} B. EDER,^{1,2} P. PUTZER,³ M. MAYERBACHER,^{1,2} N. LEMKE,³ K. U. SCHREIBER,² U. HUGENTOBLER,² AND R. KIENBERGER¹

¹Physik Department E11, Technische Universität München, Garching, Germany

²Forschungseinrichtung Satellitengeodäsie, Technische Universität München, München, Germany

³OHB System AG, Wessling, Germany

*sebastian.schweyer@ohb.de

Abstract: We demonstrate the stabilization of an all-in-fiber polarization maintaining semiconductor saturable absorber mirror (SESAM) mode locked frequency comb oscillator with an intra-cavity waveguide electro-optic phase modulator (EOM) to a narrow linewidth HeNe laser over 46 hours. The high feedback bandwidth of the EOM allows a coherent optical lock with an in-loop integrated phase noise of 1.12 rad (integrated from 10 Hz to 3 MHz) from the carrier signal. No piezo fiber stretcher was required to guarantee long-term stabilization, preventing mechanical degradation of the optical fibers and enabling a long lifetime of the oscillator. As an application a hybrid stabilization scheme is presented, where a comb tooth is phase locked to a longitudinal mode of the large ring laser "G" located at the Geodatic Observatory Wettzell. The hybrid stabilization scheme describes the optical lock of the frequency comb to the G laser and the simultaneous compensation of the ring laser frequency drift by comparing the comb repetition rate against an active H-maser reference. In this context the ring laser reached a fractional Allan deviation of $5 \cdot 10^{-16}$ at an integration time of 16384 s.

© 2018 Optical Society of America under the terms of the [OSA Open Access Publishing Agreement](#)

1. Introduction

In recent years the frequency comb evolved from a sensitive and complex laboratory breadboard setups to a compact and robust all-in-fiber system [1,2]. Frequency combs are used for demanding applications such as laser spectroscopy [3], ultra-low noise microwave signal generation [4], optical atomic clocks [5], absolute distance measurement [6] and time transfer [7]. This is due their capability of phase-coherent locking to highly stable and low noise optical and microwave references. With these capabilities frequency combs will play an important role in the future for spaceborne systems in the field of earth observation, navigation and scientific missions. In 2013 a femtosecond laser based on a semiconductor saturable absorber mirror (SESAM) was successfully tested in a low-earth orbit satellite [8,9]. In addition, a fiber comb mode-locked with a nonlinear amplifying loop mirror [10] was operated in a sounding rocket [11]. SESAM based femtosecond lasers show a robust design but are limited in terms of free-running noise due to the SESAM relaxation time [12]. In order to achieve a phase-coherent stabilization of the SESAM femtosecond laser to a narrow linewidth laser and of the laser carrier envelope offset (CEO) frequency (f_{CEO}) to a radio frequency standard, at least two fast actuators are required.

In this work, we demonstrate the phase stabilization of a SESAM-based all-in-fiber polarization maintaining (PM) Erbium oscillator with an intra-cavity waveguide electro-optic phase modulator (EOM) to an optical reference laser at 633 nm. The SESAM-based frequency comb oscillator shows a relatively high intrinsic phase noise, which leads to a free running linewidth of more than 100 kHz at the reference laser frequency. Nevertheless, a phase-coherent stabilization to the reference laser was achieved due to the high feedback bandwidth of the EOM up to the MHz

level [13] to control the repetition rate f_{rep} . Furthermore, f_{CEO} was phase stabilized with a feedback bandwidth up to 260 kHz via pump power modulation [14]. In previous works, EOMs were implemented in figure-8 [13] and nonlinear amplifying loop mirror lasers [15] as well as in Ytterbium fiber lasers [16] and in a nonlinear polarization rotation laser [14, 17, 18]. An all-in-fiber SESAM-based femtosecond Erbium laser with a waveguide EOM extends this list of frequency comb architectures.

The frequency comb presented here was stabilized to a Helium-Neon laser, which is referenced to the large ring laser gyroscope "G" at the Geodetic Observatory Wettzell [19,20]. The frequency comb and the ring laser were also referenced to an active H-maser using a hybrid stabilization approach. The aim of the hybrid stabilization approach was to compensate for drifts of the ring laser frequency, while the laser's short-term stability and low frequency noise are transferred to the frequency comb. Thereby, the ring laser benefits from the long-term stability due to the H-maser, because the phase of the backscatter coupling is stabilized. This reduces the drift of the measurements of physical effects related to variations in the Earth rotation, such as polar motion in the diurnal frequency band. In addition, the phase coherent transfer of the short-term stability to the comb modes allows the comparison of the ring laser short-term behavior against radio frequency or optical oscillators.

2. Optical setup

The fiber optical frequency comb setup is subdivided in three functional groups labelled a, b and c (see Fig. 1). The femtosecond oscillator is highlighted by the blue dotted line. Within part b, the carrier envelope offset frequency of the femtosecond oscillator is detected. In section c, the comb light is converted to 633 nm for optical stabilization to a HeNe laser [21].

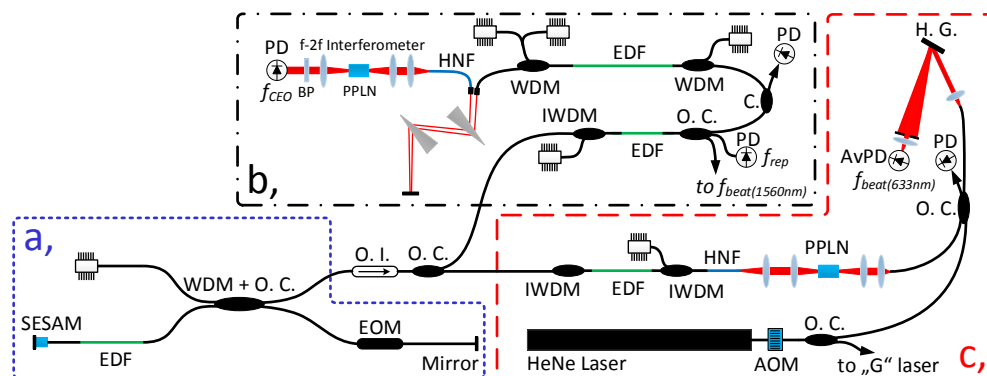


Fig. 1. Optical setup of the SESAM EOM comb including an f-2f interferometer for CEO beat detection and a 633 nm interface for optical beating with a HeNe laser. WDM, wavelength division multiplexing coupler; IWDM, WDM with integrated isolator; EDF, Erbium doped fiber; SESAM, semiconductor saturable absorber mirror; EOM, electro-optic phase modulator; O. C., optical coupler; O. I., optical isolator; C., optical circulator; BP, optical band pass filter; HNF, highly nonlinear fiber; PPLN, periodically-poled lithium niobate; H. G., holographic grating; AvPD, avalanche photo diode; PD, PiN photo-diode; AOM, acousto-optic modulator. Black solid lines indicate polarization maintaining single mode fiber.

Thus the HeNe laser is used to transfer the stability of the large ring laser "G" to the comb. The ring laser output power is 10 nW, which is not sufficient to generate an optical beat signal with the frequency comb modes. The comb oscillator (prototype laser manufactured by Toptica Photonics AG) shows a simple linear cavity design, where the pulse propagates between the saturable absorber mirror and a fiber coupled mirror. Fiber Bragg grating stabilized laser diodes at 976 nm

were used to pump the oscillator and the Erbium fiber amplifiers. The laser mode-locks at a pump threshold of 67 mW and switches to harmonic mode-locked operation above a pump power of 90 mW. Within the mode locked operation boundaries an intra-cavity soliton pulse duration between 560 fs and 390 fs is obtained. The integrated waveguide EOM has a 52 mm long lithium niobate section that allows a wide tuning of the fundamental repetition rate ($f_{rep} = 80$ MHz) by 12 Hz/V. It has a maximum tuning voltage of ± 20 V, making a slow piezo fiber stretcher unnecessary to ensure the long-term stabilization of the repetition rate. Further, the oscillator was integrated in an aluminium housing which was temperature stabilized to 25 ± 0.01 °C with a thermo-electrical cooler (TEC). The repetition rate of the femtosecond oscillator showed a sensitivity of 800 Hz/K with respect to temperature.

For the detection of f_{CEO} a common path f - $2f$ interferometer setup was used [22] consisting of a 10 mm long periodically-poled lithium niobate PPLN crystal optimized for second harmonic generation (SHG) at 2000 nm and of a Si-PIN photodiode. In order to obtain a broad and coherent supercontinuum (SC) for the f - $2f$ interferometer, the 425 fs long pulses with an energy of 6 pJ emerging from the comb oscillator, were amplified by two normal dispersion Erbium-doped fiber amplifiers. The amplified and spectrally broadened pulses were temporally compressed by a prism stage before being coupled into a 10 cm long highly nonlinear fiber (HNF). Within the HNF, a SC spectrum ranging from about 0.9 μm to 2.5 μm is generated. The average power was about 300 mW at the input of the prism stage and about 160 mW at the output of the HNF. A free running f_{CEO} beat with a signal-to-noise (SNR) of approximately 33 dB in a resolution bandwidth (RBW) of 100 kHz was obtained.

Within section c, the laser pulses were amplified by a backward pumped normal dispersion fiber amplifier. Hereby the pulses were temporally compressed within a standard PM fiber before entering the HNF. After the HNF, the dispersive-wave pulse at 1266 nm was frequency-doubled to 633 nm by a 10 mm long PPLN crystal. The pulses at 633 nm reached an average power of about 1.5 mW in a 0.5 nm spectral bandwidth. The red light from the comb and the HeNe laser (with a power of 40 μW) were superimposed in a fused fiber coupler. To achieve a perfect overlap between the transverse modes of both lasers a fiber-based solution was favored over a free space beam splitter. The optical beat f_{beat} between the HeNe laser and the frequency comb modes was detected by an avalanche photo diode. A beat signal with an SNR of approximately 35 dB in a RBW of 100 kHz was achieved. The HeNe laser (SIOS SL 04/1) laser itself was phase stabilized via a feed-forward scheme [23] to the ring laser, using an acousto-optic (AOM) as actuator. Thereby, the HeNe laser frequency was shifted by 200 ± 20 MHz to follow the G laser's frequency. The optical lock to the G laser showed an in-loop fractional Allan deviation of $3 \cdot 10^{-18}$ ($\tau = 1$ s) in relative to the HeNe laser frequency. The free running HeNe laser has a linewidth of about 1 kHz, which was estimated by the optical beat note with the ring laser.

3. Stabilization to an optical reference

The SESAM-based femtosecond laser shows a rather noisy CEO beat with a 3 dB linewidth of 2.2 MHz to 650 kHz as a function of the pump power. The linewidth of the optical beat note at 633 nm decreases from 650 kHz to 120 kHz, when increasing the pump power. The main cause for the excessive CEO noise is the high amount of anomalous net dispersion of the cavity (Gordon-Haus Jitter) [24, 25], the relative long intra-cavity pulse duration and the slow relaxation time of the SESAM [12, 26]. Measurements have shown that the 3 dB linewidth decreases almost proportionally with shorter intra-cavity pulse durations. Therefore, the oscillator was operated at a high pump power to achieve a best possible SNR and low phase noise for the CEO and optical beat signals.

The fixed point [27, 28] of the comb for pump power modulation (PPM) ranges between 150 THz and 176 THz, whereas the EOM shows a fixed point in the range of 20 THz to 30 THz. These values were obtained in our laser [29] by changing either the setpoint of the pump

power of the EOM bias voltage and simultaneously monitoring f_{rep} and f_{CEO} with a frequency counter [28]. The fixed point defines the spectral position, where no variation in the comb optical frequency is observed when changing the actuator setpoint. It is given by:

$$v_{fix(PPM,EOM)} = \left(-\Delta f_{CEO(PPM,EOM)} / \Delta f_{rep(PPM,EOM)} \right) \cdot f_{rep} + f_{CEO}$$

The EOM fixed point of about 30 THz indicates that a change in the EOM bias voltage acts much stronger on f_{rep} than on f_{CEO} compared to the effect of the pump power. For this reason $n \cdot f_{rep}$ was optically locked to the HeNe laser via the EOM bias voltage, while f_{CEO} was stabilized via pump power modulation (see Fig. 2).

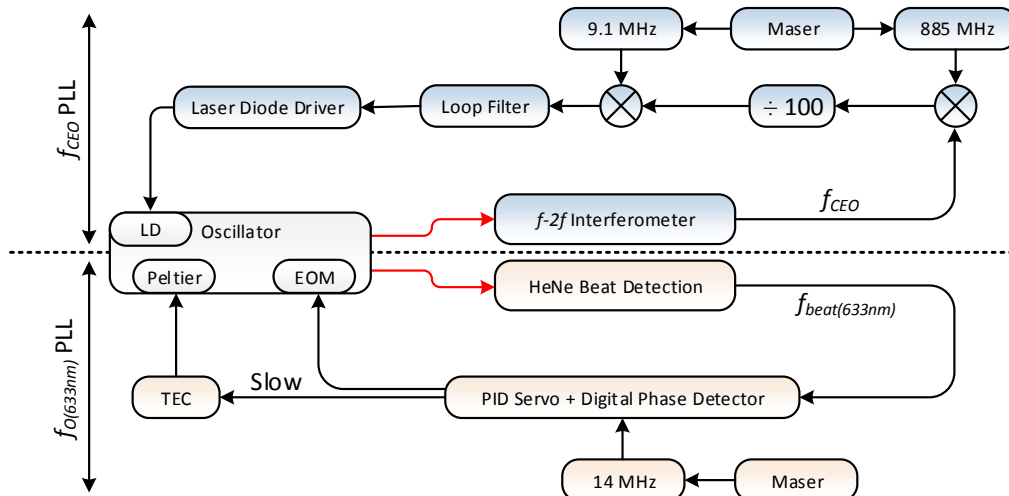


Fig. 2. Phase locked loops for stabilization of f_{CEO} and the optical beat note f_{beat}

For noisy signals a high feedback bandwidth is required to achieve coherent phase locking for both $n \cdot f_{rep}$ and f_{CEO} . The femtosecond oscillator shows a low pass filter like response in respect to pump power variations. Therefore, a feedback bandwidth of just 10 kHz was achieved when the CEO beat was stabilized with a proportional-integral controller. By the use of an active lag-lead filter in combination with a passive lead element an in-loop feedback bandwidth over 260 kHz was obtained, allowing a tight phase lock of f_{CEO} . A long-term stable lock with an analogue PLL was ensured by dividing f_{CEO} with a frequency division factor of 100, virtually enhancing the capture range of the phaselocked loop (PLL) to $\pm 100 \pi/2$ [30]. Due to the high frequency division factor it was necessary to up-convert f_{CEO} (23.5 MHz operating point) to 908 MHz by frequency mixing with a H-maser-referenced synthesizer signal at 885 MHz. The upconverted f_{CEO} signal was bandpass filtered prior to being divided to about 9.08 MHz. A home-built field programmable gate array (FPGA, Virtex 5lx30 with 250 MHz clock rate) based digital phase-frequency detector (PFD) with an integrated proportional-integral-derivative (PID) controller was used to stabilize f_{beat} via the EOM. A PFD has the advantage that it is not sensitive to amplitude fluctuations and has a higher capture range with respect to a standard analogue phase detector. Furthermore, the digital servo was used to control the setpoint of the comb temperature to achieve long-term stable operation.

3.1. Stabilization of f_{CEO}

In Fig. 3 the f_{CEO} beat is shown when locked to an H-maser referenced synthesizer. The side-bumps with a frequency offset of about 4.8 MHz from the f_{CEO} 's center frequency were also observed for the optical beat note (see Fig. 4).

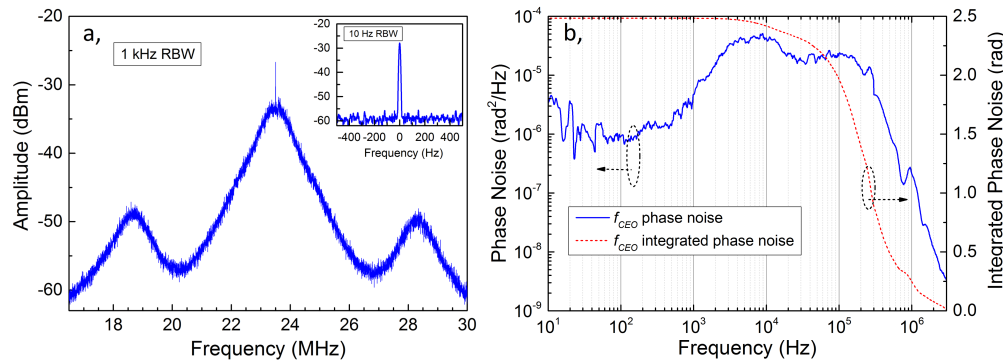


Fig. 3. Spectrum (a) and phase noise spectrum (b) of the stabilized f_{CEO} beat note.

These side-bumps did not occur due to parasitic radio frequency processes and were also observed for the free-running laser. Furthermore, the offset frequency of the side-bumps increased, when increasing the pump power to the oscillator, similar as described in [26]. The coherent peak at 23.5 MHz indicates a tight phase lock of f_{CEO} . A servo loop bandwidth of the f_{CEO} stabilization of about 260 kHz was achieved, which was estimated by the small servo bump in the phase noise spectrum. Thus the overall stabilization bandwidth was mainly limited by the modulation bandwidth of the laser diode driver. An integrated phase noise of 2.5 rad for the CEO beat note was determined integrated from 3 MHz to 10 Hz.

3.2. Stabilization of f_{beat}

Figure 4 illustrates the radio frequency spectrum and phase noise of the in-loop beat signal between the comb and the 633 nm HeNe laser.

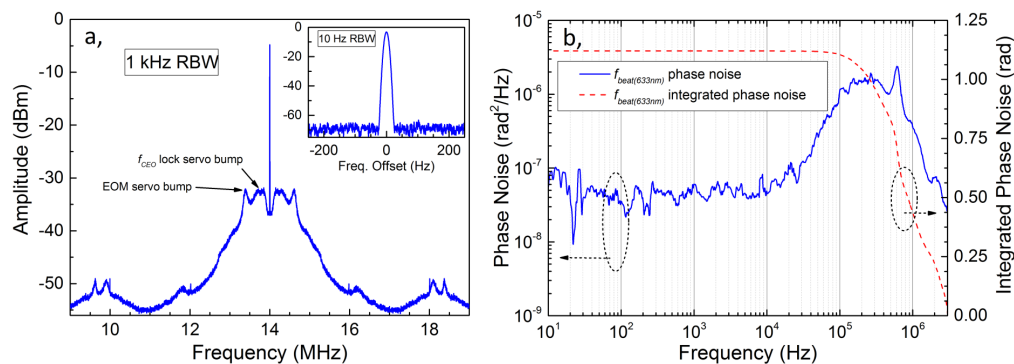


Fig. 4. Spectrum (a) and phase noise spectrum (b) of the stabilized optical f_{beat} beat note.

The coherent delta-peak at 14 MHz emerges from a U-shaped valley, which originates from the integral part of the servo loop. Hereby the integrator corner frequency was set to 100 kHz to

guarantee a robust lock by suppressing technical noise in a large bandwidth. Due to the cross influence of both servo loops a bump at 260 kHz from the delta-peak appears in the spectrum. This bump might be suppressed by introducing an electronic module to reduce the crosstalk between both feedback loops via orthogonalization. The servo bandwidth for f_{beat} stabilization was about 610 kHz and is limited by the FPGA controller. However, it was sufficient to achieve a stable phase lock with a phase noise of 1.12 rad integrated from 3 MHz to 10 Hz.

3.3. Long-term stabilization

Figure 5 shows the in-loop frequency deviation and the relative Allan deviation of f_{CEO} and f_{beat} stabilized to the HeNe transfer laser over a period longer than 46 h. The frequency stability was measured with a frequency counter (K&K FXE) in a gate time of 1 s. No phase slip was observed during the measurement. An in-loop frequency stability of 7.6 mHz ($\tau = 1$ s) and 21 mHz ($\tau = 1$ s) was observed for f_{beat} and f_{CEO} , respectively.

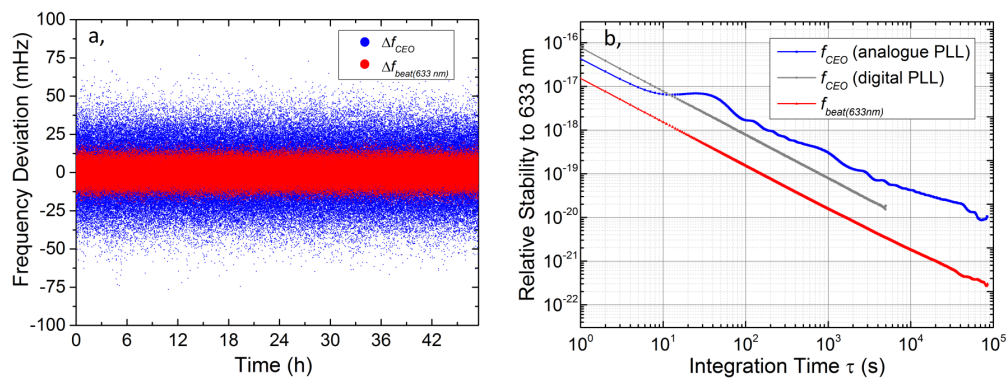


Fig. 5. (a) Frequency deviation of f_{CEO} and f_{beat} measured in a gate time of 1 s and (b) the corresponding fractional Allan deviation with respect to the HeNe laser frequency.

Also the Allan deviation of the CEO beat is illustrated, which was stabilized via the FPGA based controller in later measurements. The Allan deviation for the digital phase locked f_{beat} and f_{CEO} (digital PLL) decreases as τ^{-1} . However, the Allan deviation for f_{CEO} using the analogue PLL shows a bump for an integration time of about 30 s. It is assumed that the analogue phase locked loop is sensitive to amplitude fluctuations of the CEO beat, which could be caused by temperature and/or pump power variations.

4. Hybrid frequency comb stabilization

The G-ring laser at the Geodatic Observatory Wettzell has a 4 m squared cavity, which is mounted on a Zerodur base plate. The resonator has a total thermal expansion coefficient of less than $1 \cdot 10^{-8} \text{K}^{-1}$ and a quality factor of about $3.5 \cdot 10^{12}$ with HeNe gas as active medium all around the cavity. The laser is enclosed by a massive steel vessel in order to control the ambient air pressure around the interferometer. Until now the G-ring laser is the most sensitive laser gyroscopes to measure perturbations of Earth rotation effects, such as the polar motion, solid Earth tides, the Annual and the Chandler wobble [20]. The pressure stabilized G-ring laser resolves Earth rotation to 5 parts in 10^9 . For the optical laser frequency it delivers a relative Allan deviation of $3.65 \cdot 10^{-13}$ within an integration time of 1 s. After 2 s the frequency drift of the 16 m unstabilized cavity becomes visible (see Fig. 6(a)).

The SESAM-based comb laser was operated in Wettzell for characterization measurements of the G-ring laser in combination with a commercial Erbium fiber frequency comb system

(Menlo Systems, FC1500) [31] and an H-maser as reference. The specified Allan deviation of the H-maser as well as the estimated Allan deviation of the H-maser's signal at the ring laser laboratory are illustrated in Fig. 6(a). The H-maser's Allan deviation in the G laboratory itself was estimated in another experiment, whereby the H-maser signal was compared against a cryogenic sapphire oscillator [32]. The H-maser is located at another building at the geodetic observatory station.

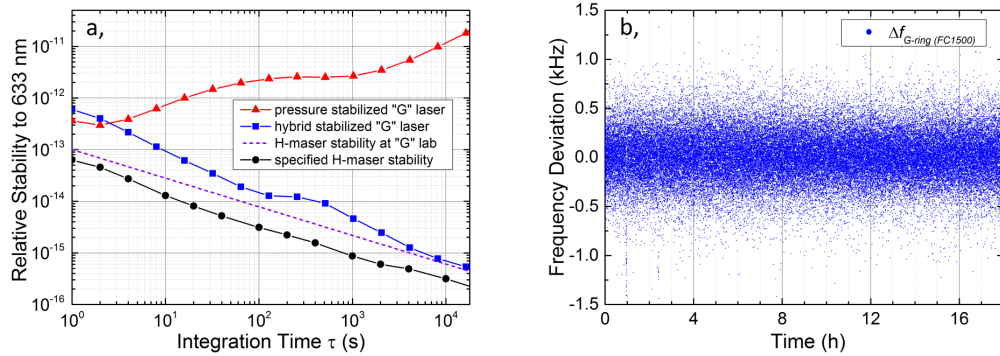


Fig. 6. (a) Allan deviation for the free-running and stabilized ring laser and for the H-maser as well as (b) Out-of-loop relative frequency stability of the hybrid stabilized "G" ring laser.

The goal was to reference the G laser to the H-maser via the SESAM-based comb to improve the laser long-term performance. In this context out-of-loop stability measurements were carried out with the commercial frequency comb. Therefore, a hybrid stabilization was established, which benefits from the short-term stability ($\tau < 2$ s) of the ring laser as well as from the long-term stability ($\tau > 2$ s) of the H-maser (see Fig. 7). Here a comb tooth was optically locked to the HeNe transfer laser, which itself was phase-stabilized to the G-ring laser. Hence, the comb tooth follows the frequency drift of the G laser and also the comb repetition rate follows the ring laser frequency in a quasi-proportional manner. The fundamental repetition rate is given as $f_{rep} = (v_G - f_{beat} - 2f_{CEO})/n$, where v_G is the ring laser frequency and n is the mode number of the referenced comb tooth. This behavior was used to phase-stabilize the ring laser and so the

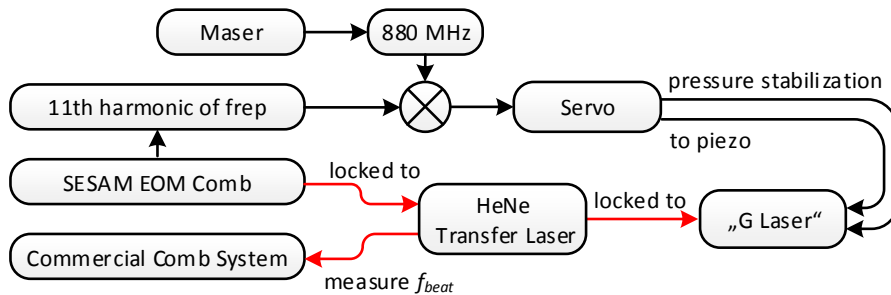


Fig. 7. Hybrid stabilization scheme for the SESAM comb laser. The SESAM comb is optically locked to the "G" ring laser, while an error signal is generated using the drift of the repetition rate of the frequency comb to stabilize the ring laser to an H-maser. The ring laser frequency is determined by a commercial frequency comb, which is fully referenced to an H-maser.

comb to an H-maser. For this, an error signal was generated by comparing the 11th harmonic of the comb's repetition rate to a synthesizer at 880 MHz referenced to the H-maser. The high

harmonic of f_{rep} was selected to magnify the absolute frequency variations by a factor of eleven compared to the fundamental repetition rate. This leads to a higher sensitivity and gain within the stabilization loop. The resulting error signal was fed to a slow servo to stabilize the ring laser frequency. The position of two cavity ring mirrors was adjusted with piezo transducers to lock the laser frequency. In addition the ambient pressure of the ring laser was controlled via the servo to guarantee a long-term stabilized ring laser.

The frequency stability of the ring laser was measured out-of-loop with the commercial frequency comb and is illustrated in Fig. 6. The ring laser shows a frequency stability of 206 Hz ($\tau = 1$ s) over a period of about 18 h. The Allan deviation of the ring laser's frequency starts at $6 \cdot 10^{-13}$ ($\tau = 1$ s), which is about twice the value of the free-running ring laser at an integration time of 1 s. However, towards a longer integration time a minimum relative frequency deviation of $5.4 \cdot 10^{-16}$ ($\tau = 16384$ s) was reached. Hereby, the ring laser frequency stability is limited by the H-maser performance itself. The bump at an integration time of 265 s was caused by the pressure stabilization.

As result, the comb adopted the short-term stability of the ring laser while showing the stability of the H-maser. Furthermore, the optical lock to the narrow linewidth ring laser allows the comparison to an ultra-stable cavity referenced laser. By this comparison the short-term stability of the G-laser could be determined, which is expected to be below the stability of the H-maser.

5. Conclusion

In this work we demonstrated the full phase stabilization of an all-in-fiber polarization maintaining SESAM-based frequency comb oscillator with an integrated waveguide EOM to a HeNe laser for over 46 hours. Despite the moderate free running phase noise of the comb, a coherent lock was achieved, by using an optimized PLL for f_{CEO} stabilization and the EOM as a fast actuator leading to in-loop servo bandwidths of up to 260 kHz and 610 kHz, respectively. An integrated phase noise for f_{CEO} of 2.5 rad and for f_{beat} of 1.12 rad was measured (integrated from 3 MHz to 10 Hz), respectively. Better results in terms of stability and noise might be obtained by a further optimization of the comb's PLLs using phase frequency detectors and a direct feedback current modulation to the cathode of the pump laser [14] for fast f_{CEO} locking. In respect to the optical lock to a HeNe laser, an in-loop stability of 7.6 mHz ($1.6 \cdot 10^{-17}$) at a gate time of 1 s was measured, which showed a τ^{-1} characteristic towards longer integration time. This performance might be sufficient for optical atomic clock applications with a stability in the range of 10^{-16} at 1 s. The here presented results point out that even SESAM mode-locked oscillators with a moderate free running linewidth of some 100's of kHz can achieve a sub-Hz stability by using an intra-cavity EOM as high speed actuator. Further, the robust all-in-fiber PM design of the oscillator opens the door to "out of lab" use. In this context, it has to be notified that the comb oscillator was recently equipped with an fiber based f-2f interferometer [33] leading to a compact and robust frequency comb design.

As an measurement application the G-ring laser was referenced to a H-maser with the SESAM-based frequency comb. The ring laser frequency was phase-locked to the H-maser for more than 16 hours via a hybrid stabilization method. Hereby, the laser overtook the H-maser long-term frequency stability showing a relative Allan deviation of $5 \cdot 10^{-16}$ in an integration time of 16384 s. This led to a significant improvement by a magnitude of four compared to the frequency stability of the free-running ring laser. In addition, the long-term hybrid stabilization shows that the SESAM-based frequency comb is a feasible tool for measurements in the radio frequency and optical domain.

Funding

Federal Ministry for Economic Affairs and Energy (BMWi) (DLR 50 NA 1301, 50 RM 1222).

Acknowledgments

We acknowledge support from the BKG. Furthermore, the author would like to thank André Gebauer (TUM-FESG), Jan Kodet (TUM-FESG), Tobias Lamour (OHB), Stéphane Schilt (University of Neuchâtel), Khanh Kieu (UA-OSC), Armin Zach (Toptica), Steve Lecomte (CSEM), Craig Benko (S2 Corporation), Hajime Inaba (AIST-JP) and Laura Sinclair (NIST) for helpful discussions. A special thanks is given to the electrical engineering students Thomas Unterholzer, Johannes Obermaier and Markus Roner for the development of laser diode drivers, temperature controllers and the FPGA based phase detector.

References

1. L. Sinclair, I. Coddington, W. Swann, G. Rieker, A. Hati, K. Iwakuni, and N. Newbury, "Operation of an optically coherent frequency comb outside the metrology lab," *Opt. Express* **22**, 6996–7006 (2014).
2. Y. Feng, X. Xu, X. Hu, Y. Liu, Y. Wang, W. Zhang, Z. Yang, L. Duan, W. Zhao, and Z. Cheng, "Environmental-adaptability analysis of an all polarization-maintaining fiber-based optical frequency comb," *Opt. Express* **23**, 17549–17559 (2015).
3. B. Bernhardt, A. Ozawa, P. Jacquet, M. Jacquy, Y. Kobayashi, T. Udem, R. Holzwarth, G. Guelachvili, T. W. Hänsch, and N. Picqué, "Cavity-enhanced dual-comb spectroscopy," *Nat. Photonics* **4**, 55–57 (2010).
4. J. Millo, M. Abgrall, M. Lours, E. M. L. English, H. Jiang, J. Guéna, A. Clairon, M. E. Tobar, S. Bize, Y. Le Coq, and G. Santarelli, "Ultralow noise microwave generation with fiber-based optical frequency comb and application to atomic fountain clock," *Appl. Phys. Lett.* **94**, 141105 (2009).
5. B. J. Bloom, T. L. Nicholson, J. R. Williams, S. L. Campbell, M. Bishof, X. Zhang, W. Zhang, S. L. Bromley, and J. Ye, "An Optical Lattice Clock with Accuracy and Stability at the 10^{-18} Level," *Nature* **506**, 71–75 (2014).
6. J. Ye, "Absolute measurement of a long, arbitrary distance to less than an optical fringe," *Opt. Lett.* **29**, 1153–1155 (2004).
7. F. R. Giorgetta, W. C. Swann, L. C. Sinclair, E. Baumann, I. Coddington, and N. R. Newbury, "Optical two-way time and frequency transfer over free space," *Nat. Photonics* **7**, 434 (2013).
8. Y. Jang, J. Lee, S. Kim, K. Lee, S. Han, Y. Kim, and S. Kim, "Space radiation test of saturable absorber for femtosecond laser," *Opt. Lett.* **39**, 2831–2834 (2014).
9. J. Lee, K. Lee, Y.-S. Jang, H. Jang, S. Han, S.-H. Lee, K.-I. Kang, C.-W. Lim, Y.-J. Kim, and S.-W. Kim, "Testing of a femtosecond pulse laser in outer space," *Sci. Rep.* **4**, 5134 (2014).
10. M. Fermann, F. Haberl, M. Hofer, and H. Hochreiter, "Nonlinear amplifying loop mirror," *Opt. Lett.* **15**, 752–754 (1990).
11. M. Lezius, T. Wilken, C. Deutsch, M. Giunta, O. Mandel, A. Thaller, V. Schkolnik, M. Schiemangk, A. Dinkelaker, A. Kohfeldt, A. Wicht, M. Krutzik, A. Peters, O. Hellmig, H. Duncker, K. Sengstock, P. Windpassinger, K. Lampmann, T. Hülsing, T. W. Hänsch, and R. Holzwarth, "Space-borne frequency comb metrology," *Optica* **3**, 1381–1387 (2016).
12. R. Paschotta, "Timing jitter and phase noise of mode-locked fiber lasers," *Opt. Express* **18**, 5041–5054 (2010).
13. E. Baumann, F. Giorgetta, J. Nicholson, W. Swann, I. Coddington, and N. Newbury, "High-performance, vibration-immune, fiber-laser frequency comb," *Opt. Lett.* **34**, 638–640 (2009).
14. K. Iwakuni, H. Inaba, Y. Nakajima, T. Kobayashi, K. Hosaka, A. Onae, and F. Hong, "Narrow linewidth comb realized with a mode-locked fiber laser using an intra-cavity waveguide electro-optic modulator for high-speed control," *Opt. Express* **20**, 13769–13776 (2012).
15. N. Kuse, J. Jiang, C. Lee, T. Schibli, and M. Fermann, "All polarization-maintaining Er fiber-based optical frequency combs with nonlinear amplifying loop mirror," *Opt. Express* **24**, 3095–3102 (2016).
16. C. Benko, A. Ruehl, M. Martin, K. Eikema, M. Fermann, I. Hartl, and J. Ye, "Full phase stabilization of a Yb: fiber femtosecond frequency comb via high-bandwidth transducers," *Opt. Lett.* **37**, 2196–2198 (2012).
17. D. Hudson, K. Holman, R. Jones, S. Cundiff, J. Ye, and D. Jones, "Mode-locked fiber laser frequency-controlled with an intracavity electro-optic modulator," *Opt. Lett.* **30**, 2948–2950 (2005).
18. Y. Nakajima, H. Inaba, K. Hosaka, K. Minoshima, A. Onae, M. Yasuda, T. Kohno, S. Kawato, T. Kobayashi, T. Katsuyama, and F. Hong, "A multi-branch, fiber-based frequency comb with millihertz-level relative linewidths using an intra-cavity electro-optic modulator," *Opt. Express* **18**, 1667–1676 (2010).
19. K. U. Schreiber, T. Klügel, J.-P. R. Wells, R. B. Hurst, and A. Gebauer, "How to Detect the Chandler and the Annual Wobble of the Earth with a Large Ring Laser Gyroscope," *Phys. Rev. Lett.*, **107** (17), p. 173904, (2011).
20. K. U. Schreiber, and J.-P. R. Wells, "Invited Review Article: Large ring lasers for rotation sensing," *Rev. Sci. Instrum.* **84**, 89 (2013).
21. Jack A. Stone and Patrick Egan, "An Optical Frequency Comb Tied to GPS for Laser Frequency/Wavelength Calibration," *J. Res. Natl. Inst. Stand. Technol.* **115**, 413–431 (2010).
22. D. J. Jones, S. A. Diddams, J. K. Ranka, A. Stentz, R. S. Windeler, J. L. Hall, and S. T. Cundiff, "Carrier-Envelope Phase Control of Femtosecond Mode-Locked Lasers and Direct Optical Frequency Synthesis," *Science* **288**, 635–639 (2000).

23. T. Sala, D. Gatti, A. Gambetta, N. Coluccelli, G. Galzerano, P. Laporta, and M. Marangoni, "Wide-bandwidth phase lock between a CW laser and a frequency comb based on a feed-forward configuration," *Opt. Lett.* **37**, 2592–2594 (2012).
24. J. Gordon and H. Haus, "Random walk of coherently amplified solitons in optical fiber transmission," *Opt. Lett.* **11**, 665–667 (1986).
25. L. Nugent-Glandorf, T. Johnson, Y. Kobayashi, and S. Diddams, "Impact of dispersion on amplitude and frequency noise in a Yb-fiber laser comb," *Opt. Lett.* **36**, 1578–1580 (2011).
26. S. Wang, S. Droste, L. Sinclair, I. Coddington, N. Newbury, T. Carruthers, and C. Menyuk, "Wake mode sidebands and instability in mode-locked lasers with slow saturable absorbers," *Opt. Lett.* **42**, 2362–2365 (2017).
27. H. R. Telle, B. Lipphardt, and J. Stenger, "Kerr-lens, mode-locked lasers as transfer oscillators for optical frequency measurements," *Appl. Phys. B* **74**, 1–6 (2002).
28. B. Washburn, W. Swann, and N. Newbury, "Response dynamics of the frequency comb output from a femtosecond fiber laser," *Opt. Express* **13**, 10622–10633 (2005).
29. S. Schweyer, R. Kienberger, B. Eder, P. Putzer, A. Kölnberger, and N. Lemke, "Characterization of a SESAM mode-locked erbium fiber laser frequency comb with an integrated electro-optic modulator," *Proc. EFTF Conf.* 189–192 (2014).
30. E. N. Ivanov, F.-X. Esnault, and E. A. Donley, "Offset phase locking of noisy diode lasers aided by frequency division," *Review of Scientific Instruments* **82**, 083110 (2011).
31. K. Schreiber, A. Gebauer, and J. Wells, "Closed-loop locking of an optical frequency comb to a large ring laser," *Opt. Lett.* **38**, 3574–3577 (2013).
32. S. Grop, P.-Y. Bourgeois, N. Bazin, Y. Kersalé, E. Rubiola, C. Langham, M. Oxborrow, D. Clapton, S. Walker, J. D. Vicente, and V. Giordano, "A cryocooled 10 GHz oscillator with 10^{-15} frequency stability," *Rev. of Sci. Instrum.* **81**, 025102 (2010).
33. L. C. Sinclair, J.-D. Deschenes, L. Sonderhouse, W. C. Swann, I. H. Khader, E. Baumann, N. R. Newbury, and I. Coddington, "Invited Article: A compact optically coherent fiber frequency comb," *Rev. Sci. Instrum.* **86**, 081301 (2015).